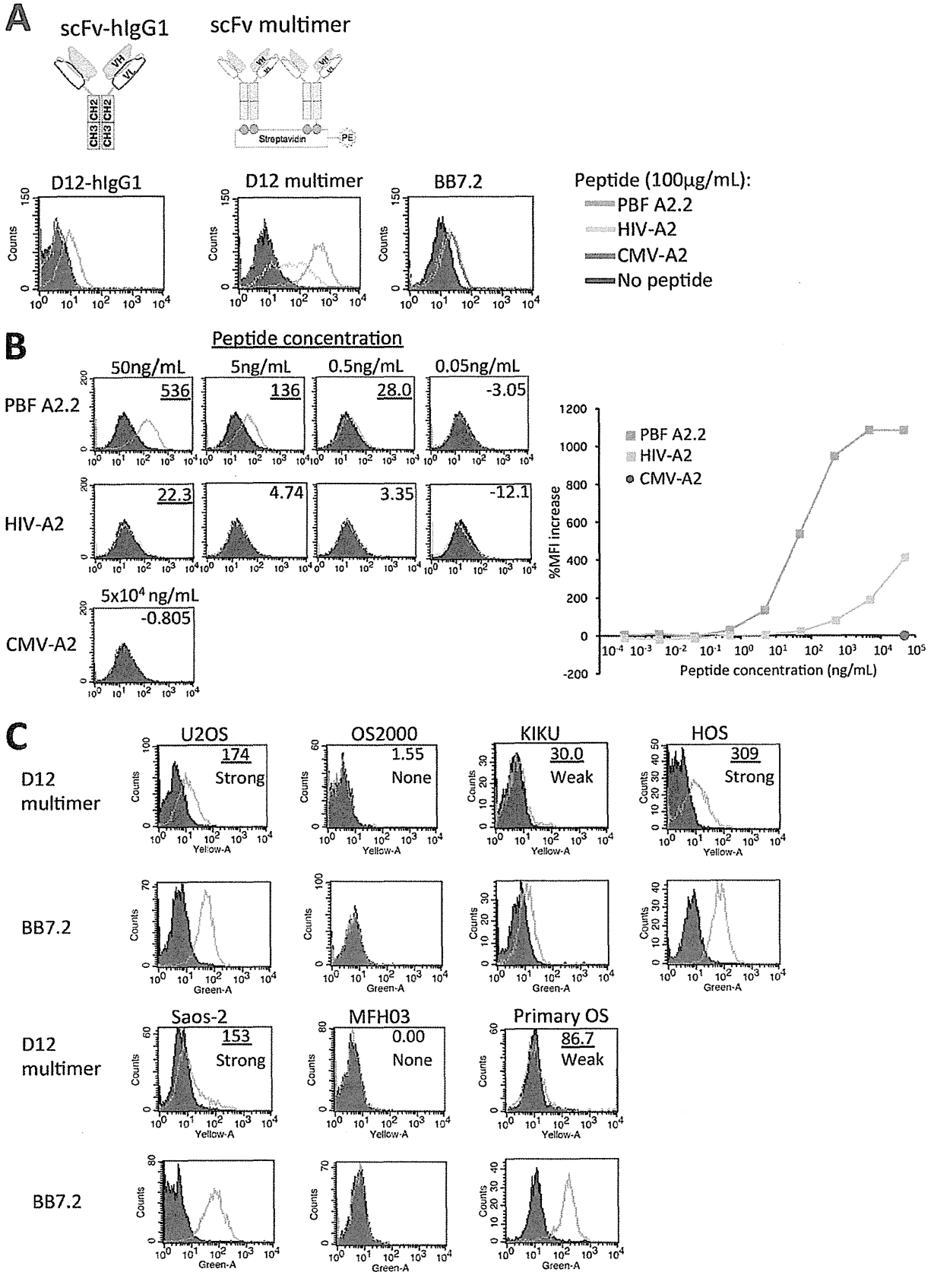
A
scFv-hIgG1
scFv multimer
VH
VL
CH2
CH3
Streptavidin
PE
D12-hIgG1
D12 multimer
BB7.2
Counts
Peptide (100μg/mL):
PBF A2.2
HIV-A2
CMV-A2
No peptide
B
Peptide concentration
50ng/mL
5ng/mL
0.5ng/mL
0.05ng/mL
PBF A2.2
536
136
28.0
-3.05
HIV-A2
22.3
4.74
3.35
-12.1
5x10⁴ ng/mL
CMV-A2
-0.805
%MFI increase
Peptide concentration (ng/mL)
C
U2OS
174
Strong
OS2000
1.55
None
KIKU
30.0
Weak
HOS
309
Strong
D12 multimer
BB7.2
Saos-2
153
Strong
MFH03
0.00
None
Primary OS
86.7
Weak
Yellow-A
Green-A

TABLE 2
FACS analysis of peptide-pulsed T2 cells

Peptide concentration (ng/mL)		50000	5000	500	50	5	0.5	0.05	0.005	0.0005	0.00005	0.000005	0
PBF A2.2	MFI	280	279	248	150	55.7	30.2	22.9	25.6	25.0	24.7	26.0	23.6
	%MFI increase	1085	1084	950	536	136	28.0	-3.05	8.30	5.84	4.57	10.2	
HIV-A2	MFI	121	68.1	42.4	28.9	24.7	24.4	20.8	19.3	21.2	24.7	25.1	23.4
	%MFI increase	413	188	79.4	22.3	4.74	3.35	-12.1	-18.4	-10.4	4.53	6.18	
CMV-A2	MFI	23.4											
	%MFI increase	-0.805											

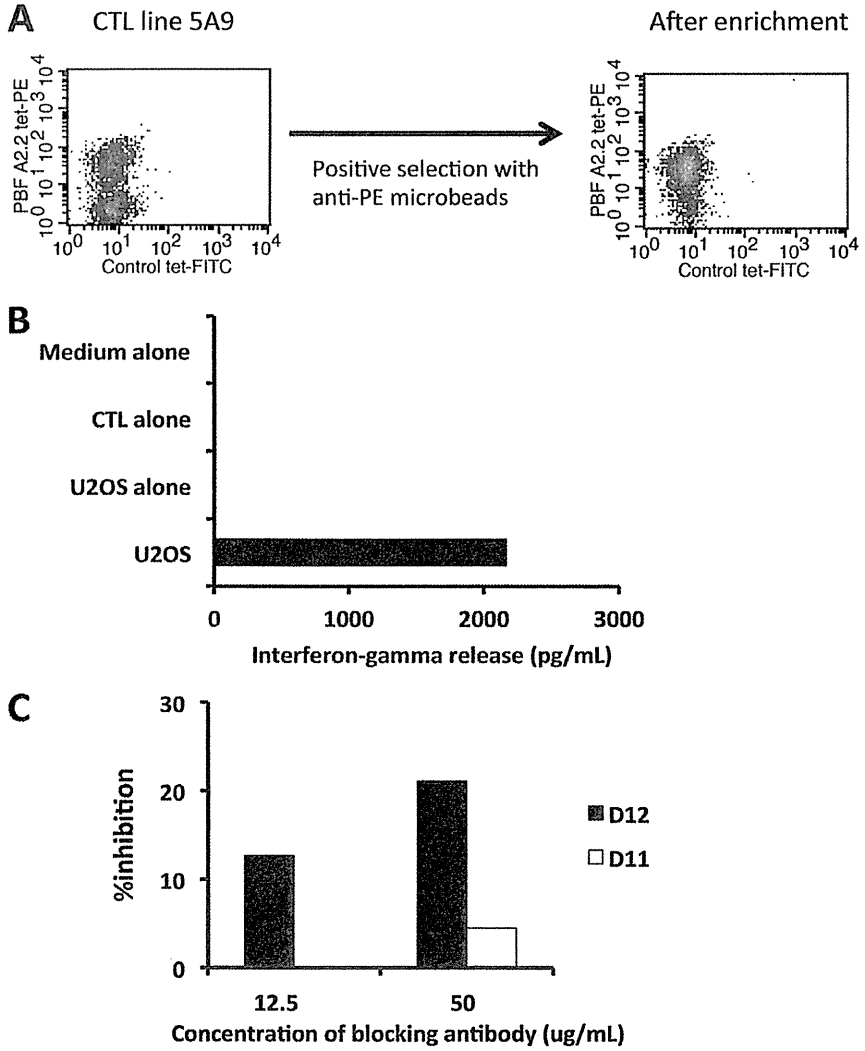

FIGURE 6. **Clone scFv D12 showed specificity similar to natural CTL recognizing HLA-A*02:01·PBF A2.2 peptide complex.** *A*, tetramer staining of oligoclonal CTL line 5A9 directed to HLA-A*02:01·PBF A2.2 peptide before and after positive selection. *B*, CTL response against U2OS cells assessed by ELISA. Tetramer-positive cells after enrichment were used as the responder. *C*, inhibition effect of scFv-hIgG1 on CTL response. scFv D12-hIgG1 and irrelevant scFv D11-hIgG1 were used as blocking antibodies. The inhibition effect on CTL response was calculated as described under "Experimental Procedures."

change of HLA-A*02:01 molecules induced by the binding of peptides into the binding groove of the HLA. However, the reactivity of the multimer against peptide PBF A2.2 was 100-fold higher than for peptide HIV-A2. In addition, the observation that scFv clone D12 could weakly react with primary OS cells highly expressing HLA-A*02:01 suggested that the cross-

FIGURE 5. **scFv clone D12 could recognize PBF A2.2 peptide presented on the surface of sarcoma cells.** *A* and *B*, FACS analysis of reactivity of D12 scFv-hIgG1 (1 mg/ml) and D12 scFv multimer (10 μg/ml) against T2 cells pulsed with the indicated peptides. %MFI increase is indicated. T2 without peptide was used as the negative control. A more than 20.0% MFI increase is indicated by *underlining*. *C*, FACS analysis of the reactivity of the D12 scFv multimer (3 μg/ml) with sarcoma cell lines and primary culture cells. Osteosarcoma cell line U2OS (A*02:01/A*3201, PBF+), OS2000 (A*2402, PBF+), KIKU (A*0206/A*2402, PBF+), HOS (A*02:11, PBF+), Saos-2 (A*02:01/A*24:02, PBF+), malignant fibrous histiocytoma cell line MFH2003 (A*2402, PBF−), and primary culture of osteosarcoma (*Primary OS*; A*02:01, PBF+) were used as target cells. A more than 20.0% MFI increase is indicated by *underlining*. The expression status of HLA-A2·PBF A2.2 peptide complex was graded as follows: strong (≥100% MFI increase), weak (≥20% but <100% MFI increase), and none (<20% MFI increase).

reactivity of the clone against the other endogenous peptides was very low. The strong expression status of the HLA-A*02:01·PBF A2.2 peptide complex on U2OS cells is a rare condition. However, Michaeli *et al.* (32) reported that the tyrosinase(369–377) peptide was highly expressed on HLA-A2+ melanoma cells.

For specificity, the ideal probe that reacts with a naturally presented HLA·peptide complex is soluble TCR isolated from a specific CTL clone. We have established several CTL clones that react with tumor-associated antigens. Nevertheless, establishment of CTL clones is still difficult. In contrast, the technique using a scFv phage display library can provide scFv mimicking TCR specificity for a short time. The finding that scFv D12 could partially inhibit the reactivity of a CTL clone directed to the HLA-A*02:01·PBF A2.2 peptide complex suggested that scFv D12 recognized the near part of the HLA·peptide complex docked with TCR of the CTL clone.

Conversely, the advantage of using antibodies for probing HLA·peptide complexes is that they show high affinity on the nanomolar or picomolar order (28). The affinity range of natural TCRs binding to HLA class I·peptides is a K_D value of $1–50 \times 10^{-6}$ M. The affinity of scFv D12 was 3 orders of magnitude greater than that of standard TCRs (33).

The phage display library in the present study was constructed from naïve donors. Therefore, the library could be useful to select specific scFvs that react with the other HLA·tumor-associated antigens. We previously identified various CTL epitopes of tumor-associated antigens and cancer stemlike cell/cancer-initiating cell-associated antigens (12, 13, 20, 34–40). It is also very attractive to identify scFv clones recognizing the CTL epitopes derived from these antigens in the context of HLA-A24 or HLA-A2 for the assessment of the expression status on other tumor cells.

In conclusion, we isolated scFv clone D12, which reacted with the HLA-A*02:01·PBF A2.2 peptide complex presented on osteosarcoma cells. This clone might be useful to detect the HLA·peptide complex on sarcoma cells for selection of patients and prediction of the efficacy of PBF A2.2 peptide-based immunotherapy. In the future, the clone might also be useful for antibody-based immunotherapy and adoptive cell transfer therapy using genetically engineered lymphocytes expressing chimeric antigenic receptors.

Acknowledgments—We thank Dr. Hideo Takasu (Dainippon Sumitomo Pharma Co., Ltd., Osaka, Japan) for the kind donation of synthetic peptides and Dr. Shigeru Takamoto (Japanese Red Cross Hokkaido Block Blood Center, Sapporo, Japan) for the kind donation of human sera.

REFERENCES

1. Ferrari, S., and Palmerini, E. (2007) Adjuvant and neoadjuvant combination chemotherapy for osteogenic sarcoma. *Curr. Opin. Oncol.* **19,** 341–346
2. The Japanese Orthopaedic Association (JOA) Musculoskeletal Tumor Committee (2000) *General Rules for Clinical and Pathological Studies on Malignant Bone Tumors*, pp. 52–61, 3rd Ed., Kanabara, Tokyo
3. Southam, C. M., Marcove, R. C., Levin, A. G., Buchsbaum, H. J., and Miké, V. (1972) Proceedings: clinical trial of autogenous tumor vaccine for treatment of osteogenic sarcoma. *Proc. Natl. Cancer Conf.* **7,** 91–100
4. Campbell, C. J., Cohen, J., and Enneking, W. F. (1975) Editorial: new therapies for osteogenic sarcoma. *J. Bone Joint Surg. Am.* **57,** 143–144
5. Kawaguchi, S., Wada, T., Tsukahara, T., Ida, K., Torigoe, T., Sato, N., and Yamashita, T. (2005) A quest for therapeutic antigens in bone and soft tissue sarcoma. *J. Transl. Med.* **3,** 31
6. Lewis, V. O. (2007) What's new in musculoskeletal oncology. *J. Bone Joint Surg. Am.* **89,** 1399–1407
7. Meyers, P. A., Schwartz, C. L., Krailo, M., Kleinerman, E. S., Betcher, D., Bernstein, M. L., Conrad, E., Ferguson, W., Gebhardt, M., Goorin, A. M., Harris, M. B., Healey, J., Huvos, A., Link, M., Montebello, J., Nadel, H., Nieder, M., Sato, J., Siegal, G., Weiner, M., Wells, R., Wold, L., Womer, R., and Grier, H. (2005) Osteosarcoma: a randomized, prospective trial of the addition of ifosfamide and/or muramyl tripeptide to cisplatin, doxorubicin, and high-dose methotrexate. *J. Clin. Oncol.* **23,** 2004–2011
8. Maki, R. G. (2006) Future directions for immunotherapeutic intervention against sarcomas. *Curr. Opin. Oncol.* **18,** 363–368
9. Sato, N., Hirohashi, Y., Tsukahara, T., Kikuchi, T., Sahara, H., Kamiguchi, K., Ichimiya, S., Tamura, Y., and Torigoe, T. (2009) Molecular pathological approaches to human tumor immunology. *Pathol. Int.* **59,** 205–217
10. Tsukahara, T., Torigoe, T., Tamura, Y., Wada, T., Kawaguchi, S., Tsuruma, T., Hirata, K., Yamashita, T., and Sato, N. (2008) Antigenic peptide vaccination: provoking immune response and clinical benefit for cancer. *Curr. Immunol. Rev.* **4,** 235–241
11. Boeckle, S., Pfister, H., and Steger, G. (2002) A new cellular factor recognizes E2 binding sites of papillomaviruses which mediate transcriptional repression by E2. *Virology* **293,** 103–117
12. Tsukahara, T., Nabeta, Y., Kawaguchi, S., Ikeda, H., Sato, Y., Shimozawa, K., Ida, K., Asanuma, H., Hirohashi, Y., Torigoe, T., Hiraga, H., Nagoya, S., Wada, T., Yamashita, T., and Sato, N. (2004) Identification of human autologous cytotoxic T-lymphocyte-defined osteosarcoma gene that encodes a transcriptional regulator, papillomavirus binding factor. *Cancer Res.* **64,** 5442–5448
13. Tsukahara, T., Kawaguchi, S., Torigoe, T., Kimura, S., Murase, M., Ichimiya, S., Wada, T., Kaya, M., Nagoya, S., Ishii, T., Tatezaki, S., Yamashita, T., and Sato, N. (2008) Prognostic impact and immunogenicity of a novel osteosarcoma antigen, papillomavirus binding factor, in patients with osteosarcoma. *Cancer Sci.* **99,** 368–375
14. Fletcher, C. D. M., van den Berg, E., and Molenaar, W. M. (2002) in *World Health Organization Classification of Tumors* (Fletcher, C. D. M., Unni, K. K., and Mertens, F., eds) pp. 120–122, IARC Press, Lyon, France
15. Sichtig, N., Silling, S., and Steger, G. (2007) Papillomavirus binding factor (PBF)-mediated inhibition of cell growth is regulated by 14-3-3β. *Arch. Biochem. Biophys.* **464,** 90–99
16. Tsukahara, T., Kimura, S., Ichimiya, S., Torigoe, T., Kawaguchi, S., Wada, T., Yamashita, T., and Sato, N. (2009) Scythe/BAT3 regulates apoptotic cell death induced by papillomavirus binding factor in human osteosarcoma. *Cancer Sci.* **100,** 47–53
17. Jordanovski, D., Herwartz, C., Pawlowski, A., Taute, S., Frommolt, P., and Steger, G. (2013) The hypoxia-inducible transcription factor ZNF395 is controlled by IκB kinase-signaling and activates genes involved in the innate immune response and cancer. *PLoS One* **8,** e74911
18. Hasegawa, R., Tomaru, Y., de Hoon, M., Suzuki, H., Hayashizaki, Y., and Shin, J. W. (2013) Identification of ZNF395 as a novel modulator of adipogenesis. *Exp. Cell Res.* **319,** 68–76
19. Tsukahara, T., Kawaguchi, S., Torigoe, T., Asanuma, H., Nakazawa, E., Shimozawa, K., Nabeta, Y., Kimura, S., Kaya, M., Nagoya, S., Wada, T., Yamashita, T., and Sato, N. (2006) Prognostic significance of HLA class I expression in osteosarcoma defined by anti-pan HLA class I monoclonal antibody, EMR8-5. *Cancer Sci.* **97,** 1374–1380
20. Tsukahara, T., Kawaguchi, S., Torigoe, T., Takahashi, A., Murase, M., Kano, M., Wada, T., Kaya, M., Nagoya, S., Yamashita, T., and Sato, N. (2009) HLA-A*0201-restricted CTL epitope of a novel osteosarcoma antigen, papillomavirus binding factor. *J. Transl. Med.* **7,** 44
21. Nabeta, Y., Kawaguchi, S., Sahara, H., Ikeda, H., Hirohashi, Y., Goroku, T., Sato, Y., Tsukahara, T., Torigoe, T., Wada, T., Kaya, M., Hiraga, H., Isu, K., Yamawaki, S., Ishii, S., Yamashita, T., and Sato, N. (2003) Recognition by cellular and humoral autologous immunity in a human osteosarcoma cell line. *J. Orthop. Sci.* **8,** 554–559

22. Wada, T., Uede, T., Ishii, S., Matsuyama, K., Yamawaki, S., and Kikuchi, K. (1988) Monoclonal antibodies that detect different antigenic determinants of the same human osteosarcoma-associated antigen. *Cancer Res.* **48,** 2273–2279
23. Tsukahara, T., Kawaguchi, S., Ida, K., Kimura, S., Tamura, Y., Ikeda, T., Torigoe, T., Nagoya, S., Wada, T., Sato, N., and Yamashita, T. (2006) HLA-restricted specific tumor cytolysis by autologous T-lymphocytes infiltrating metastatic bone malignant fibrous histiocytoma of lymph node. *J. Orthop. Res.* **24,** 94–101
24. Pansri, P., Jaruseranee, N., Rangnoi, K., Kristensen, P., and Yamabhai, M. (2009) A compact phage display human scFv library for selection of antibodies to a wide variety of antigens. *BMC Biotechnol.* **9,** 6
25. Schofield, D. J., Pope, A. R., Clementel, V., Buckell, J., Chapple, S. D., Clarke, K. F., Conquer, J. S., Crofts, A. M., Crowther, S. R., Dyson, M. R., Flack, G., Griffin, G. J., Hooks, Y., Howat, W. J., Kolb-Kokocinski, A., Kunze, S., Martin, C. D., Maslen, G. L., Mitchell, J. N., O'Sullivan, M., Perera, R. L., Roake, W., Shadbolt, S. P., Vincent, K. J., Warford, A., Wilson, W. E., Xie, J., Young, J. L., and McCafferty, J. (2007) Application of phage display to high throughput antibody generation and characterization. *Genome Biol.* **8,** R254
26. Lefranc, M. P. (2003) IMGT, the international ImMunoGeneTics database. *Nucleic Acids Res.* **31,** 307–310
27. Nahshol, O., Bronner, V., Notcovich, A., Rubrecht, L., Laune, D., and Bravman, T. (2008) Parallel kinetic analysis and affinity determination of hundreds of monoclonal antibodies using the ProteOn XPR36. *Anal. Biochem.* **383,** 52–60
28. Dahan, R., and Reiter, Y. (2012) T-cell-receptor-like antibodies—generation, function and applications. *Expert Rev. Mol. Med.* **14,** e6
29. Purbhoo, M. A., Sutton, D. H., Brewer, J. E., Mullings, R. E., Hill, M. E., Mahon, T. M., Karbach, J., Jäger, E., Cameron, B. J., Lissin, N., Vyas, P., Chen, J. L., Cerundolo, V., and Jakobsen, B. K. (2006) Quantifying and imaging NY-ESO-1/LAGE-1-derived epitopes on tumor cells using high affinity T cell receptors. *J. Immunol.* **176,** 7308–7316
30. Bossi, G., Gerry, A. B., Paston, S. J., Sutton, D. H., Hassan, N. J., and Jakobsen, B. K. (2013) Examining the presentation of tumor-associated antigens on peptide-pulsed T2 cells. *Oncoimmunology* **2,** e26840
31. Parker, K. C., Bednarek, M. A., and Coligan, J. E. (1994) Scheme for ranking potential HLA-A2 binding peptides based on independent binding of individual peptide side-chains. *J. Immunol.* **152,** 163–175
32. Michaeli, Y., Denkberg, G., Sinik, K., Lantzy, L., Chih-Sheng, C., Beauverd, C., Ziv, T., Romero, P., and Reiter, Y. (2009) Expression hierarchy of T cell epitopes from melanoma differentiation antigens: unexpected high level presentation of tyrosinase-HLA-A2 complexes revealed by peptide-specific, MHC-restricted, TCR-like antibodies. *J. Immunol.* **182,** 6328–6341
33. van der Merwe, P. A., and Davis, S. J. (2003) Molecular interactions mediating T cell antigen recognition. *Annu. Rev. Immunol.* **21,** 659–684
34. Hirohashi, Y., Torigoe, T., Maeda, A., Nabeta, Y., Kamiguchi, K., Sato, T., Yoda, J., Ikeda, H., Hirata, K., Yamanaka, N., and Sato, N. (2002) An HLA-A24-restricted cytotoxic T lymphocyte epitope of a tumor-associated protein, survivin. *Clin. Cancer Res.* **8,** 1731–1739
35. Sato, Y., Nabeta, Y., Tsukahara, T., Hirohashi, Y., Syunsui, R., Maeda, A., Sahara, H., Ikeda, H., Torigoe, T., Ichimiya, S., Wada, T., Yamashita, T., Hiraga, H., Kawai, A., Ishii, T., Araki, N., Myoui, A., Matsumoto, S., Umeda, T., Ishii, S., Kawaguchi, S., and Sato, N. (2002) Detection and induction of CTLs specific for SYT-SSX-derived peptides in HLA-A24$^+$ patients with synovial sarcoma. *J. Immunol.* **169,** 1611–1618
36. Ida, K., Kawaguchi, S., Sato, Y., Tsukahara, T., Nabeta, Y., Sahara, H., Ikeda, H., Torigoe, T., Ichimiya, S., Kamiguchi, K., Wada, T., Nagoya, S., Hiraga, H., Kawai, A., Ishii, T., Araki, N., Myoui, A., Matsumoto, S., Ozaki, T., Yoshikawa, H., Yamashita, T., and Sato, N. (2004) Crisscross CTL induction by SYT-SSX junction peptide and its HLA-A*2402 anchor substitute. *J. Immunol.* **173,** 1436–1443
37. Hariu, H., Hirohashi, Y., Torigoe, T., Asanuma, H., Hariu, M., Tamura, Y., Aketa, K., Nabeta, C., Nakanishi, K., Kamiguchi, K., Mano, Y., Kitamura, H., Kobayashi, J., Tsukahara, T., Shijubo, N., and Sato, N. (2005) Aberrant expression and potency as a cancer immunotherapy target of inhibitor of apoptosis protein family, Livin/ML-IAP in lung cancer. *Clin. Cancer Res.* **11,** 1000–1009
38. Honma, I., Torigoe, T., Hirohashi, Y., Kitamura, H., Sato, E., Masumori, N., Tamura, Y., Tsukamoto, T., and Sato, N. (2009) Aberrant expression and potency as a cancer immunotherapy target of α-methylacyl-coenzyme A racemase in prostate cancer. *J. Transl. Med.* **7,** 103
39. Inoda, S., Morita, R., Hirohashi, Y., Torigoe, T., Asanuma, H., Nakazawa, E., Nakatsugawa, M., Tamura, Y., Kamiguchi, K., Tsuruma, T., Terui, T., Ishitani, K., Hashino, S., Wang, Q., Greene, M. I., Hasegawa, T., Hirata, K., Asaka, M., and Sato, N. (2011) The feasibility of Cep55/c10orf3 derived peptide vaccine therapy for colorectal carcinoma. *Exp. Mol. Pathol.* **90,** 55–60
40. Morita, R., Nishizawa, S., Torigoe, T., Takahashi, A., Tamura, Y., Tsukahara, T., Kanaseki, T., Sokolovskaya, A., Kochin, V., Kondo, T., Hashino, S., Asaka, M., Hara, I., Hirohashi, Y., and Sato, N. (2014) Heat shock protein DNAJB8 is a novel target for immunotherapy of colon cancer-initiating cells. *Cancer Sci.* **105,** 389–395

Laboratory Investigation (2014) 94, 1355–1369

Fibroblasts induce expression of FGF4 in ovarian cancer stem-like cells/cancer-initiating cells and upregulate their tumor initiation capacity

Kazuyo Yasuda[1], Toshihiko Torigoe[1], Tasuku Mariya[1,2], Takuya Asano[1,2], Takafumi Kuroda[2], Junichi Matsuzaki[1], Kanae Ikeda[3], Makoto Yamauchi[3], Makoto Emori[1], Hiroko Asanuma[4], Tadashi Hasegawa[4], Tsuyoshi Saito[2], Yoshihiko Hirohashi[1] and Noriyuki Sato[1]

Cancer stem-like cells (CSCs)/cancer-initiating cells (CICs) are defined as a small population of cells within cancer that contribute to cancer initiation and progression. Cancer-associated fibroblasts (CAFs) are stromal fibroblasts surrounding tumor cells, and they have important roles in tumor growth and tumor progression. It has been suggested that stromal fibroblasts and CSCs/CICs might mutually cooperate to enhance their growth and tumorigenic capacity. In this study, we investigated the effects of fibroblasts on tumor-initiating capacity and stem-like properties of ovarian CSCs/CICs. CSCs/CICs were isolated from the ovarian carcinoma cell line HTBoA as aldehyde dehydrogenase 1 high ($ALDH1^{high}$) population by the ALDEFLUOR assay. Histological examination of tumor tissues derived from $ALDH1^{high}$ cells revealed few fibrous stroma, whereas those derived from fibroblast-mixed $ALDH1^{high}$ cells showed abundant fibrous stroma formation. *In vivo* tumor-initiating capacity and *in vitro* sphere-forming capacity of $ALDH1^{high}$ cells were enhanced in the presence of fibroblasts. Gene expression analysis revealed that fibroblast-mixed $ALDH1^{high}$ cells had enhanced expression of fibroblast growth factor 4 (FGF4) as well as stemness-associated genes such as *SOX2* and *POU5F1*. Sphere-forming capacity of $ALDH1^{high}$ cells was suppressed by small-interfering RNA (siRNA)-mediated knockdown of FGFR2, the receptor for FGF4 which was expressed preferentially in $ALDH1^{high}$ cells. Taken together, the results indicate that interaction of fibroblasts with ovarian CSCs/CICs enhanced tumor-initiating capacity and stem-like properties through autocrine and paracrine FGF4-FGFR2 signaling.

Laboratory Investigation (2014) **94,** 1355–1369; doi:10.1038/labinvest.2014.122; published online 20 October 2014

Tumors are composed of morphologically and phenotypically heterogeneous cells that are derived from a small subpopulation of pluripotent stem-like cancer cells (cancer stem cell hypothesis).[1–3] Cancer stem-like cells (CSCs) are also named as cancer-initiating cells (CICs) since they possess high tumorigenic capacity *in vivo*. With recent progress in this research field, CSCs/CICs have been isolated by several methods.[4] CSCs/CICs are now defined as a small population of cancer cells that have (1) high tumor-initiating capacity, (2) self-renewal capacity and (3) differentiation potential. Since CSCs/CICs are resistant to conventional cancer therapies including chemotherapy, radiotherapy and some molecular targeting therapies, they are thought to be responsible for disease recurrence and distant metastasis.[5] CSCs/CICs have phenotypic properties similar to those of normal stem cells; however, the molecular mechanisms underlying their high tumorigenic capacity, a hallmark of CSCs/CICs, are still elusive.

Tumor microenvironments have important roles in cancer progression.[6] They are composed of cancer cells and surrounding stromal elements, such as blood vessels, inflammatory cells and fibroblasts, which are termed as cancer-associated fibroblasts (CAFs).[7] CAFs are activated fibroblasts that can be identified by immunohistochemical staining using anti-α-smooth muscle actin (α-SMA).[8,9] These fibroblasts are also known as reactive fibroblasts, peri-tumor fibroblasts and

[1]Department of Pathology, Sapporo Medical University School of Medicine, Sapporo, Japan; [2]Department of Obstetrics and Gynecology, Sapporo Medical University School of Medicine, Sapporo, Japan; [3]Department of Plastic and Reconstructive Surgery, Sapporo Medical University School of Medicine, Sapporo, Japan and [4]Department of Surgical Pathology, Sapporo Medical University School of Medicine, Sapporo, Japan
Correspondence: Dr K Yasuda, MD, PhD or Dr T Torigoe, MD, PhD or Dr Y Hirohashi, MD, PhD, Department of Pathology, Sapporo Medical University School of Medicine, South-1 West-17, Chuo-Ku, Sapporo 060-8556, Japan.
E-mail: yasudasann@gmail.com, torigoe@sapmed.ac.jp or hirohash@sapmed.ac.jp

Received 25 February 2014; revised 5 August 2014; accepted 18 August 2014

myofibroblasts.[10] CAFs are observed in various types of malignancies including gastric cancer, ovarian cancer and breast cancer. In many cases, tumors with abundant CAFs have a poorer prognosis than those of tumors with less CAFs, since CAFs have significant roles in the tumor microenvironment for promotion of cell growth and invasion.[11,12] It has also been suggested that CSCs/CICs might preferentially interact with CAFs, which serve as a niche in the CSC/CIC microenvironment.[13]

In this study, we show evidence that fibroblasts can induce expression of stemness-associated genes and fibroblast growth factor 4 (FGF4) in ovarian carcinoma CSCs/CICs, leading enhancement of tumor-initiating capacity. Our study highlights the significance of FGF4-FGFR2 signaling induced by the interaction between fibroblasts and CSCs/CICs in the tumor microenvironment.

MATERIALS AND METHODS

Cell Culture

The experiments were conducted with the approval of the Sapporo Medical University Study Review Board. The human ovarian carcinoma cell line HTBoA was previously established from an ovarian anaplastic carcinoma.[14] Human primary skin fibroblasts N25-5 and N30-3 were prepared from normal skin tissues of two Japanese patients who underwent plastic surgery after obtaining informed consent, in compliance with the ethical guidelines of Sapporo Medical University School of Medicine. All cells were maintained in Dulbecco's modified Eagle's medium (DMEM; Sigma-Aldrich, St Louis, MO, USA) supplemented with 10% FBS in a 5% CO_2 incubator at 37 °C.

ALDEFLUOR Assay

An ALDEFLUOR assay kit was purchased from Stem Cell Technologies (Vancouver, BC, Canada) and used according to the manufacturer's recommendations. Briefly, 10^6 cells were suspended in 1 ml assay buffer containing 1.5 mM of an ALDH1 substrate, BODIPY®-aminoacetaldehyde (BAAA), and incubated for 50 min at 37 °C. An inhibitor of ALDH1, diethylamino-benzaldehyde (DEAB), at a 10-fold molar excess was used as a negative control. Flow cytometry and cell sorting were performed using a FACS Aria II cell sorter (BD Biosciences, Bedford, MA, USA).

In Vivo Tumor Formation Assay

The experiments were conducted with the approval of the Sapporo Medical University Study Review Board. $ALDH1^{high}$ cells and $ALDH1^{low}$ cells isolated from HTBoA cells were resuspended at 10^2–10^4 cells in 50 μl of PBS and mixed with 50 μl of matrigel (BD Biosciences). The cell-matrigel mixture suspension was subcutaneously injected in the dorsum of 6-week-old non-obese diabetic/severe combined immunodeficiency (NOD/SCID) mice (NOD.CB17-Prdkcscid/J, Charles River Laboratory, Yokohama, Japan) under anesthesia. Tumor growth was monitored weekly, and tumor volume was calculated by $XY^2/2$ (X = long axis, Y = short axis). For a fibroblast mixture study, 10^4 of $ALDH1^{high}$ cells or $ALDH1^{low}$ cells were mixed with 10^4 of fibroblasts and suspended in 100 μl of PBS matrigel mixture. Tumor growth was monitored weekly.

Sphere Formation Assay

$ALDH1^{high}$ cells and $ALDH1^{low}$ cells were isolated from HTBoA cells and incubated in CSC Certified™, Complete Serum-Free Medium (Cell Systems Corporation, Kirkland, WA, USA) using six-well ultra-low attachment plates (Corning, Corning, NY, USA). One thousand cells were seeded in each well, and the total number of spheres was counted 2 weeks after incubation. For a fibroblast mixture study, 10^3 of fibroblasts were mixed with 10^3 of $ALDH1^{high}$ cells or $ALDH1^{low}$ cells, and then the same sphere culture procedure was performed. Human recombinant FGF4 (Wako Pure Chemical Industries, Osaka, Japan) was added to the sphere formation assay culture medium to a final concentration of 0.2 ng/ml. Fibroblast culture supernatant was obtained from fibroblast culture in CSC Certified™, Complete Serum-Free Medium after 2 days of culture. The supernatant was added to the sphere culture medium to a final concentration of 50%.

Immunohistochemical Staining

Human leukocyte antigen (HLA) immunostaining was performed using mouse monoclonal anti-HLA class I antibody (clone: EMR8-5) as described previously.[15] The monoclonal antibody was used at 1 μg/ml. α-SMA staining, FGF4 staining and FGFR2 staining were done using rabbit polyclonal anti-alpha smooth muscle actin antibody (Abcam, Cambridge, MA, USA), anti-FGF4 antibody (Abcam) and anti-FGFR2 antibody (Abcam). The antibodies were used at 1 μg/ml.

RT-PCR Analysis

Total RNA was reverse-transcribed using Superscript II reverse transferase enzyme (Life Technologies, Grand Island, NY, USA). PCR was performed using Taq polymerase (Qiagen, Valencia, CA, USA). The thermal cycling conditions were 94 °C for 2 min followed by 35 cycles of 15 s at 94 °C, 30 s at 60 °C and 30 s at 72 °C. Primer pairs used for RT-PCR analysis were 5′-TGTTAGCTGATGCCGACTTG-3′ and 5′-TTCTTAGCCCGCTCAACACT-3′ for *ALDH1A1* with an expected PCR product size of 154 base pairs (bps), 5′-GCCTGGGCGCCGAGTGGA-3′ and 5′-GGGCGAGCCGTTCATGTAGGTCTG-3′ for *SOX2* with an expected PCR product size of 301 bps, 5′-AGGTGTTCAGCCAAACGACC-3′ and 5′-TGATCGTTTGCCCTTCTGGC-3′ for *POU5F1 (Oct3/4)* with an expected PCR product size of 161 bps, 5′-ATCCAGCTTGTCCCCAAAG-3′ and 5′-ATTTCATTCGCTGGTTCTGG-3′ for *NANOG* with an expected PCR product size of 459 bps, 5′-AGGCTGGGAGCCAAATGAAG-3′ and 5′-TGTGGTCAAAAGCCCGTGG-3′ for *CD44* with an expected PCR product size of 83 bps, 5′-ATTTCATTGCTCCTGGGCG-3′

and 5′-GCATACGTATTATAGCCCA-3′ for *FGF3* with an expected PCR product size of 642 bps, 5′-TGAGTGCACGTT CAAGGAGA-3′ and 5′-GAGGAAGTGGGTGACCTTCA-3′ for *FGF4* with an expected PCR product size of 154 bps, 5′-CCCGGATGGCAAAGTCAATGG-3′ and 5′-TTCAGGGC AACATACCACTCCCG-3′ for *FGF5* with an expected PCR product size of 230 bps, 5′-CACGAGGAGAACCCCTACA-3′ and 5′-TCCCTTGGTACAAGTCTGA-3′ for *FGF6* with an expected PCR product size of 335 bps, 5′-GTGGAAAAGAAC GGCAGTAAATACG-3′ and 5′-CACCATACAGGCGATTAAG AAGACC-3′ for *FGFR2* with an expected PCR product size of 69 bps, 5′-ATGAGCAACTGCAGCATCAC-3′ and 5′-GGAG AAGCAGCATCTTCCAG-3′ for *TGFB1* with an expected PCR product size of 150 bps, 5′-CCCTGGCTACCTGAG TGAAG-3′ and 5′-GGCTCGCAGTAGGTAACTGG-3′ for *SMAD2* with an expected PCR product size of 252 bps, 5′-AACTCTTGGGACCTGGTGTG-3′ and 5′-GTCCTTCTCC ACCCAAGTGA-3′ for *STAT3* with an expected PCR product size of 269 bps, 5′-GCTGAGGAAGATGCTGGTTC-3′ and 5′-TCTTTCAACACGCAGGACAG-3′ for *IL-1B* with an expected PCR product size of 248 bps, and 5′-ACCACAG TCCATGCCATCAC-3′ and 5′-TCCACCACCCTGTTGCTG TA-3′ for *glyceraldehyde-3-phosphate dehydrogenase* (*GAPDH*) with an expected product size of 452 bps. *GAPDH* was used as an internal control.

Quantitative Real-Time PCR Analysis (qPCR)

Quantitative real-time PCR was performed using the ABI PRISM 7000 Sequence Detection System (Applied Biosystems, Foster City, CA, USA) according to the manufacturer's protocol. *ALDH1A1* (Hs00946916_m1), *SOX2* (Hs01053049_s1), *POU5F1* (Hs00999632_g1), *NANOG* (Hs04260366_g1), *CD44* (Hs01075861_m1), *DNAJB8* (Hs00542087_s1) primers and probes were designed by the manufacturer (TaqMan Gene expression assays; Applied Biosystems). Thermal cycling was performed using 40 cycles of 95 °C for 15 s followed by 60 °C for 1 min. Each experiment was done in triplicate, and normalized to the *GAPDH* gene as an internal control.

Gene Knockdown of *FGFR2* with Small-Interfering RNA

FGFR2 small-interfering RNAs (siRNAs) (SiHK0771) (Sigma, Tokyo, Japan) were used to knockdown FGFR2 mRNA. Transfection of siRNA duplexes was performed with Lipofectamine RNAimax (Life Technologies) according to the manufacturer's manual. Gene knockdown was confirmed by RT-PCR.

Statistical Analysis

Statistical analysis, data fitting and graphics were performed by the SPSS software package ver.19 (SPSS, Chicago, IL, USA). Data were shown as the mean ± s.d. of at least three independent experiments and Student's *t*-test was used to assess the statistical significant difference ($P<0.05$). Overall survival (OS), which was defined as interval from the date of first diagnosis to the date of death of disease progression, and progression-free survival (PFS), interval from the date of first diagnosis to the date of disease progression, were estimated using Kaplan–Meier method and compared with the log-rank test. The relevance with *FGF4* expression was analyzed by Pearson's χ-square tests. Correlation coefficient between

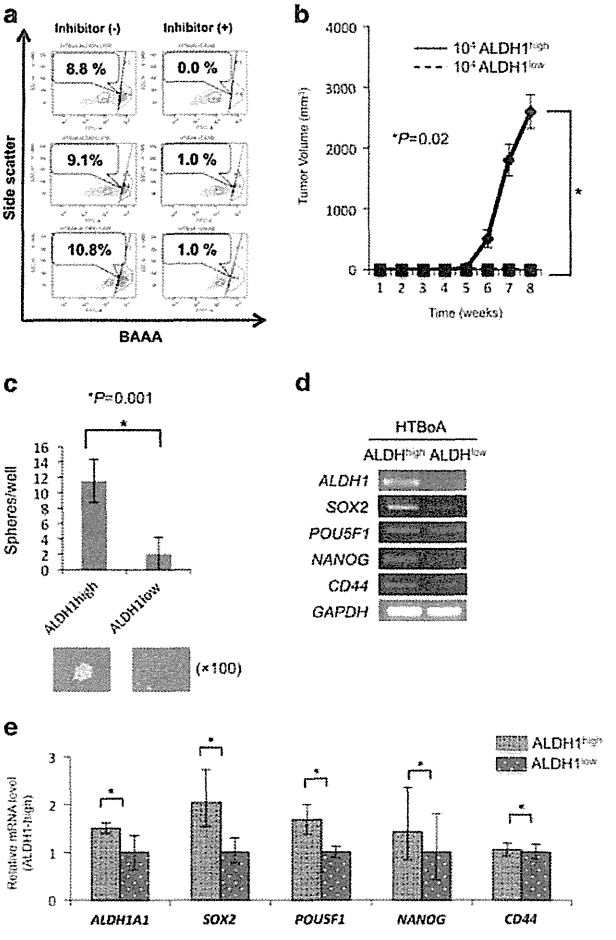

Figure 1 ALDH1^{high} cells of HTBoA have cancer stem-like properties. (**a**) Detection of ALDH1^{high} cells by ALDEFLUOR assay. HTBoA ovarian adenocarcinoma cells were stained with BAAA and analyzed by a flow cytometer. The percentage represents the ratio of ALDH^{high} cells. (**b**) Tumor formation assay of ALDH1^{high} and ALDH1^{low} cells of HTBoA. 1×10^4 ALDH1^{high} cells and 1×10^4 ALDH1^{low} cells were inoculated subcutaneously into the backs of NOD/SCID mice. Tumor volume was measured weekly. Data represent means ± s.d. Differences between ALDH1^{high} and ALDH1^{low} cells were examined for statistical significance using Student's *t*-test. *P-values. (**c**) Sphere formation assay. Numbers of spheres from ALDH1^{high} and ALDH1^{low} cells were counted on day 7. Data represent means ± s.d. The differences were examined for statistical significance using Student's t-test. *P-values. Representative sphere pictures are shown in the right panel (× 100). (**d**) RT-PCR for stem cell markers. Expression of stem cell marker genes was analyzed by RT-PCR. GAPDH was used as an internal control. High: ALDH1^{high} cells, low: ALDH1^{low} cells. (**e**) Quantitative real-time PCR for stem cell markers. Expression of stem cell marker genes was analyzed by quantitative real-time PCR.

FGF4 expression level and CAFs ratio was analyzed in Excel 2010. Each multivariate analysis was performed with the stepwise method. In all analysis, *P*-values <0.05 were considered as statistically significant.

RESULTS

CSCs/CICs are Enriched in the ALDH1^{high} Population of Ovarian Carcinoma HTBoA Cells

Several methods for isolating CSCs/CICs, including Hoechst33342 assay, ALDEFLUOR assay and use of cell surface markers (ie, CD44 and CD133), have been reported.[4] In our previous study, we found that CSCs/CICs of ovarian carcinoma MCAS cells were enriched in an aldehyde dehydrogenase high activity population (ALDH1^{high}) by the ALDEFLUOR assay as well as in a side population by the Hoechst33342 assay.[16,17] Therefore, we sorted out ALDH1^{high} cells and ALDH1^{low} cells from ovarian carcinoma HTBoA cells by the ALDEFLUOR assay (Figure 1a). The ratio of ALDH1^{high} cells was 8.8–10.8% in three independent experiments. ALDH1^{high} cells exhibited significantly higher tumor-forming ability (3 of 5 mice) than did ALDH1^{low} cells (0 of 5 mice) when they were inoculated into NOD/SCID mice (Figure 1b; Table 1). ALDH1^{high} cells exhibited significantly higher sphere-forming capacity in culture with serum-free medium (Figure 1c) and higher expression levels of stem cell markers (SOX2, POU5F1, NANOG and CD44) than did ALDH1^{low} cells (Figures 1d and e). These results indicate that CSCs/CICs of HTBoA cells are enriched in ALDH1^{high} cells.

Table 1 Tumor-initiating capacity of HTBoA ovarian cancer cells

	Number of mice with tumor formation[a]/ Total number of mice (injected cell number)		
Cells	10^2	10^3	10^4
HTBoA			
ALDH1^{high} cells	0/5	0/5	3/5
ALDH1^{low} cells	0/5	0/5	0/5

[a]Tumor formation was evaluated at day 70 post inoculation.

Normal Fibroblasts Enhanced the Tumorigenic Capacity and CAF Induction in CSC/CIC-Derived Tumors of HTBoA Cells

It has been reported that CAFs could induce epithelial–mesenchymal transition and cancer stemness in prostate carcinoma PC3 cells.[18] We therefore examined whether fibroblasts can affect the tumorigenic capacity of CSCs/CICs of ovarian cancer cells. Ten thousand ALDH1^{high} cells with or without a mixture of normal skin fibroblasts (N25-5) were inoculated into NOD/SCID mice (Figure 2a). Fibroblast-mixed ALDH1^{high} cells showed a higher tumor incidence (5 of 5) and formed significantly larger tumors than did ALDH1^{high} cells without a mixture of fibroblasts (Figure 2b; Table 2). Neither ALDH1^{low} only cells nor fibroblast-mixed ALDH1^{low} cells exhibited tumor formation in five mice (Table 2). Histological examination revealed that fibroblast-mixed ALDH1^{high} tumor tissues contained abundant fibrous stroma, whereas ALDH1^{high} only tumor tissues contained few stroma (Figures 2c and d). The stromal fibroblasts were negative for HLA class I and positive for α-SMA by immunohistochemical examination, indicating that they were CAFs derived from recipient mouse (Figure 2d). Similar results were confirmed by the experiments using another fibroblasts (N30-3) (Supplementary Figure 1). Next, we examined *in vitro* sphere formation capacity of ALDH1^{high} and ALDH1^{low} cells in the presence or absence of fibroblasts (Figure 3). ALDH1^{high} cells exhibited significantly higher sphere formation capacity in the presence of fibroblasts than those without fibroblasts or ALDH1^{low} cells. Mixture of fibroblasts could not enhance the sphere formation capacity of ALDH1^{low} cells. SMA-positive fibroblasts were observed in peripheral region of the spheres derived from HTBoA mixed with fibroblasts. These data indicate that normal fibroblasts promote the tumor-initiating capacity and CAF induction capacity of CSCs/CICs, but not those of non-CSCs/CICs.

Cancer Stemness Genes were Upregulated in a Fibroblast-Mixed ALDH1^{high} Tumor

Tumor-initiating capacity, as determined by an *in vivo* tumor formation assay and an *in vitro* sphere formation assay, is a hallmark of CSCs/CICs and is closely associated with the expression of cancer stemness genes such as SOX2, POU5F1 and NANOG. DNAJB8 is a newly identified CSC-related gene that controls tumor-initiating ability in renal CSCs.[19]

Figure 2 *In vivo* tumor formation assay of ALDH1^{high} cells in the presence or absence of fibroblasts. (**a**) Schema of cell transplantation into NOD/SCID mice. 1×10^4 ALDH1^{high} cells with or without a mixture of 1×10^4 human normal skin fibroblasts (N25-5) were suspended in 100 μl of PBS matrigel mixture and inoculated into NOD/SCID mice. (**b**) Tumor formation assay. Fibroblast-mixed ALDH1^{high} cells developed earlier and significantly larger tumors than did ALDH1^{high} only cells. Data represent means ± s.d. Differences between fibroblast-mixed ALDH1^{high} tumor and ALDH1^{high} only tumor were examined for statistical significance using Student's t-test. **P*-values. (**c**) HE staining of ALDH1^{high} only tumor. Representative picture of hematoxylin and eosin staining of tumor tissue. × 200 magnification. (**d**) HE staining and immunostaining of fibroblast-mixed ALDH1^{high} tumor. Upper panel: Representative picture of hematoxylin and eosin staining of the tumor tissue. Abundant CAFs are induced in tumor tissue. × 100 magnification. Middle panel: Immunostaining with anti-HLA class I antibody. Tumor cells are positive for HLA, but stromal cells are negative. × 100 magnification. Lower panel: Immunostaining with anti-α-SMA antibody. Stromal fibroblasts are positive for α-SMA. × 100 magnification.

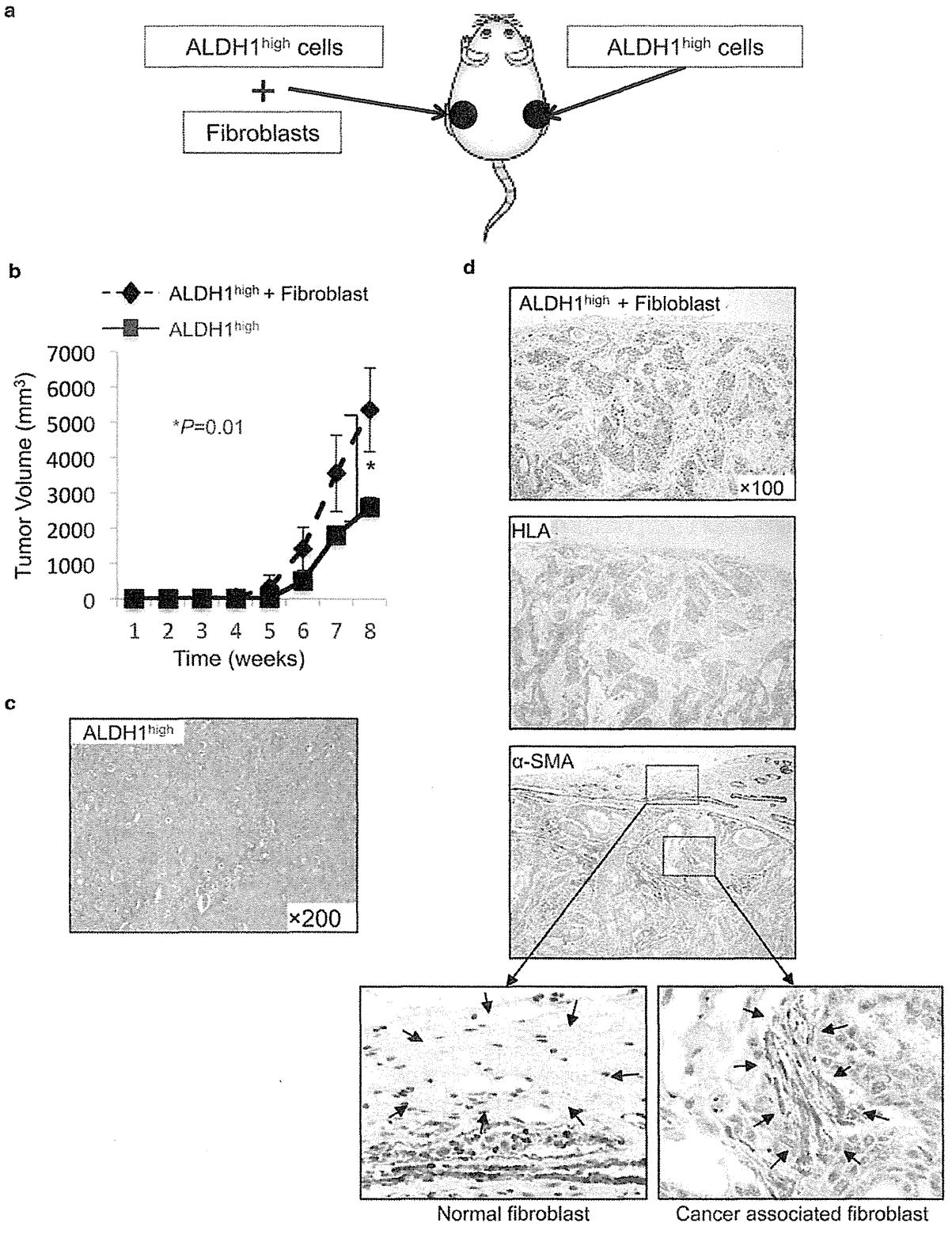
a
ALDH1high cells
+
Fibroblasts
ALDH1high cells
b
ALDH1high + Fibroblast
ALDH1high
Tumor Volume (mm3)
7000
6000
5000
4000
3000
2000
1000
0
*P=0.01
*
1 2 3 4 5 6 7 8
Time (weeks)
c
ALDH1high
×200
d
ALDH1high + Fibloblast
×100
HLA
α-SMA
Normal fibroblast
Cancer associated fibroblast

Table 2 Tumor-initiating capacity of HTBoA cells in the presence or absence of fibroblasts

Cells	Number of mice with tumor formation[a]/Total number of mice
Fibroblast-mixed ALDH1^{high} cells	5/5
ALDH1^{high} cells	3/5
Fibroblast-mixed ALDH1^{low} cells	0/5
ALDH1^{low} cells	0/5
Fibroblasts	0/5

10^4 tumor cells were inoculated with or without a mixture of 10^4 fibroblasts.
[a]Tumor formation was evaluated at day 70 post inoculation.

Therefore, expression levels of these cancer stemness genes were examined by quantitative real-time PCR. CSC/CIC-related genes were upregulated in fibroblast-mixed ALDH1^{high} tumors (Figure 4a). Protein levels of SOX2 and ALDH1 were also increased in fibroblast-mixed ALDH1^{high} tumor tissues as detected by immunohistochemical staining (Figure 4b).

FGF4 Gene Expression was Induced in ALDH1^{high} Cells after Mixing with Fibroblasts

To determine the differences between gene expression in CSC/CIC-derived tumors with CAFs (fibroblast-mixed ALDH1^{high} tumors) and those without CAFs (ALDH1^{high} only tumors), comparative gene expression analysis was performed by RT-PCR. Previous report presented that FGF family might be involved with stromal induction of cancer.[20] The expression levels of four FGF family genes (FGF3, FGF4, FGF5 and FGF6) that are related to oncogenesis were addressed, in tumor samples derived from fibroblast-mixed ALDH1^{high} cells, and only ALDH1^{high} cells (Figure 5a). Fibroblast line cells were also used as a control. FGF3, FGF5 and FGF6 were undetectable in tumors derived from fibroblast-mixed ALDH1^{high} cells, and only ALDH1^{high} cells. Whereas, FGF4 was detected in tumor derived from fibroblast-mixed ALDH1^{high} cells; however, FGF4 was undetectable in tumor derived from only ALDH1^{high} cells. The data suggested that *FGF4* was a candidate for stromal induction. *FGF4* is not only a growth factor for fibroblasts but also an oncogenic growth factor that has potential to transform mice embryonal fibroblasts.[21] Therefore, we further analyzed the expression levels of *FGF4* and its related genes by RT-PCR. As shown in Figure 5b, expression of *FGF4* was upregulated in fibroblast (N25-5)-mixed ALDH1^{high} tumors compared with the expression in ALDH1^{high} only tumors. Similar results were obtained from another fibroblast (N30-3)-mixed ALDH1^{high} tumor (Supplementary Figure 1). The expression levels of *FGF4* receptor (*FGFR2*), TGF-β signaling molecules (*TGFB1* and *SMAD2*) and inflammatory signaling molecules (*IL-1B* and *STAT3*) were also higher in fibroblast-mixed ALDH1^{high} tumors than in ALDH1^{high} only tumors. *FGF4* gene expression level was also increased after co-culture of ALDH1^{high} cells with fibroblasts, although *FGFR2* expression level was not changed (Figure 5c). In contrast to ALDH1^{high} cells, ALDH1^{low} cells barely expressed *FGFR2*, and *FGF4* gene expression was not detected even after co-culture with fibroblasts (Figure 5c). In Figure 5d, positivity to anti-*FGF4* and anti-*FGFR2* antibody was extremely high in tumors derived from fibroblast-mixed ALDH1^{high} cells compared with that in tumors derived from ALDH1^{high} cells.

FGF4-FGFR2 Signaling has an Important Role in the Sphere-Forming Capacity of Fibroblast-Mixed ALDH1^{high} Cells

To determine the significance of *FGF4* gene expression in the mechanism of fibroblast-induced cancer stemness in ALDH1^{high} cells, we examined the sphere-forming capacity in the presence of recombinant human *FGF4*. *FGF4* significantly enhanced the sphere-forming capacity of ALDH1^{high} cells but not that of ALDH1^{low} cells (Figure 6a). These results are consistent with the findings that the *FGF4* receptor is expressed on ALDH1^{high} cells but is expressed at a very low level on ALDH1^{low} cells (Figure 5c). Next, we examined the effect of *FGFR2* knockdown on the sphere-forming capacity of ALDH1^{high} cells in the presence or absence of fibroblasts. The sphere-forming capacity of ALDH1^{high} cells was dramatically suppressed by knockdown of *FGFR2* even in the absence of fibroblasts (Figure 6b). These results indicate that *FGFR2* is crucial not only for the fibroblast-induced sphere-forming capacity of CSCs/CICs but also for the basal sphere-forming capacity in the absence of fibroblasts. *FGFR2* is known to function as a receptor for several FGF family growth factors. Indeed, the sphere culture medium contained *FGF2* (*bFGF*), for which *FGFR2* acts as a receptor.

Soluble Factors Released from Fibroblasts can Promote the Sphere-Forming Capacity of ALDH1^{high} Cells

To determine whether cell-to-cell contact is required for the promotion of sphere formation, we collected fibroblast culture supernatant and examined the activity. Normal human fibroblasts were cultured in CSC Certified^{TM}, Complete Serum-Free Medium for 2 days. Then, the supernatant was added to the sphere culture. As shown in Figure 7, fibroblast culture supernatant enhanced the sphere-forming capacity of ALDH1^{high} cells but not that of ALDH1^{low} cells. These results indicate that cell-to-cell contact between fibroblasts and CSCs/CICs is not required and that soluble factors released from fibroblasts have activity for enhancing the sphere formation capacity of CSCs/CICs of HTBoA cells.

High Expression Levels of *FGF4* are Associated with Poor Prognosis

A total 122 of epithelial ovarian cancer tissues were immunohistochemically stained with anti-*FGF4* antibody and counted the positivity of staining. We divided into three groups

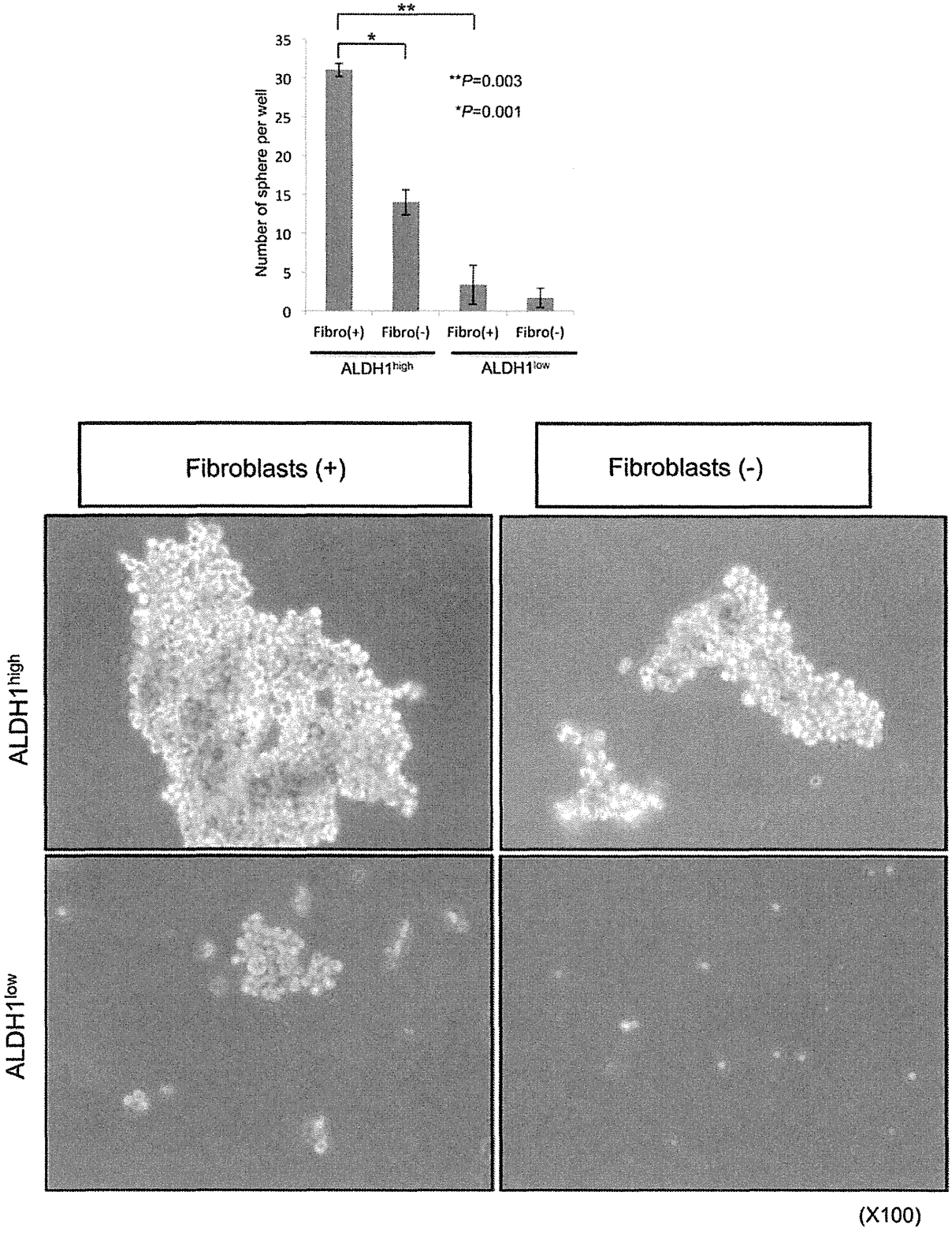

Figure 3 Sphere formation assay in the presence or absence of fibroblasts. Sphere numbers of four groups (fibroblast-mixed ALDH1^{high} cells, ALDH1^{high} only cells, fibroblast-mixed ALDH1^{low} cells, ALDH1^{low} only cells) were evaluated at day 7. Data represent means ± s.d. The differences were examined for statistical significance using Student's *t*-test. **P*-values. Representative sphere pictures are shown in the lower panel (× 100).

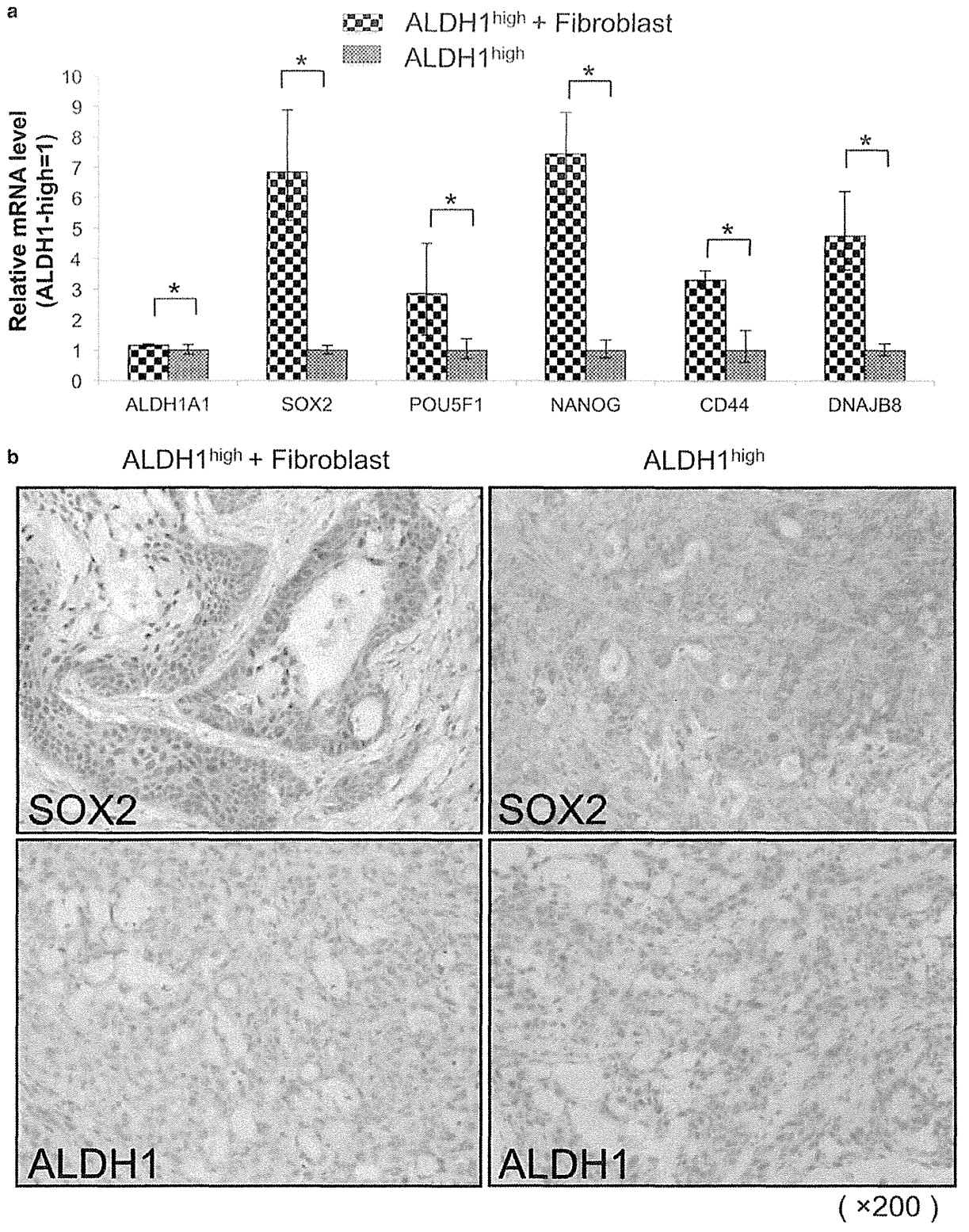

Figure 4 *RT-PCR and immunostaining of tumor tissues.* (**a**). *Quantitative real-time PCR for stem cell markers. Expression of stem cell marker genes was* analyzed by RT-PCR. GAPDH was used as an internal control. (**b**) Immunostaining for SOX2 and ALDH1. SOX2 (upper panels) and ALDH1 (lower panels) were detected by immunostaining with specific antibodies. × 200 magnification.

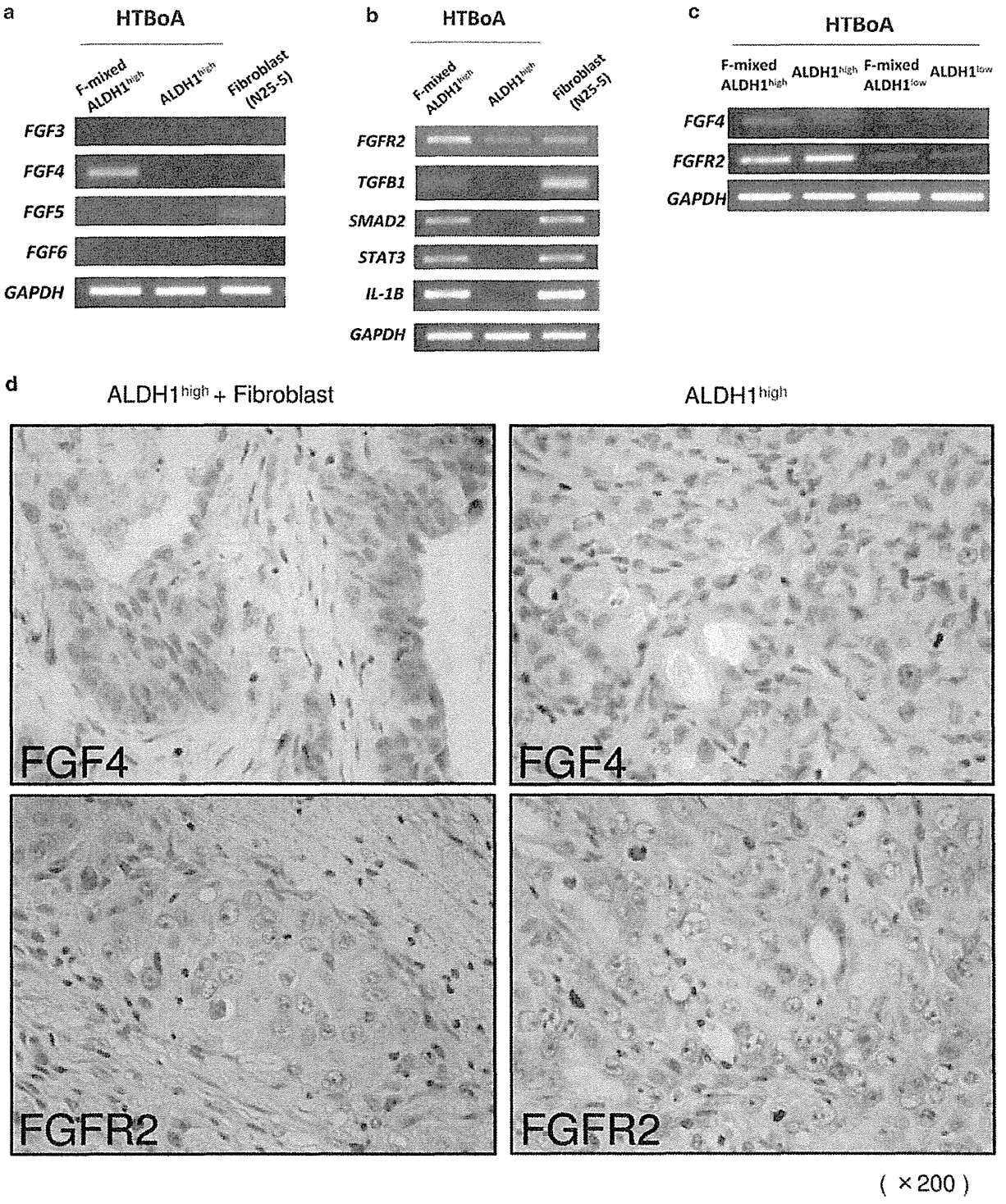

Figure 5 RT-PCR for FGF4 and its related genes. (**a**) Gene expression analysis of FGF family. Gene expression in tumor samples and normal skin fibroblasts was analyzed by RT-PCR. GAPDH was used as an internal control. (**b**) Gene expression analysis with tumor samples and fibroblasts. Gene expression in tumor samples and normal skin fibroblasts was analyzed by RT-PCR. GAPDH was used as an internal control. (**c**) Gene expression analysis with *in vitro* cultured cells. Gene expression in four groups of *in vitro* cultured cells (fibroblast-mixed ALDH1^{high} cells, ALDH1^{high} only cells, fibroblast-mixed ALDH1^{low} cells, ALDH1^{low} only cells) was analyzed by RT-PCR. GAPDH was used as an internal control. (**d**) Immunostaining for FGF4 and FGFR2. FGF4 (upper panels) and FGFR2 (lower panels) were detected by immunostaining with specific antibodies. × 200 magnification.

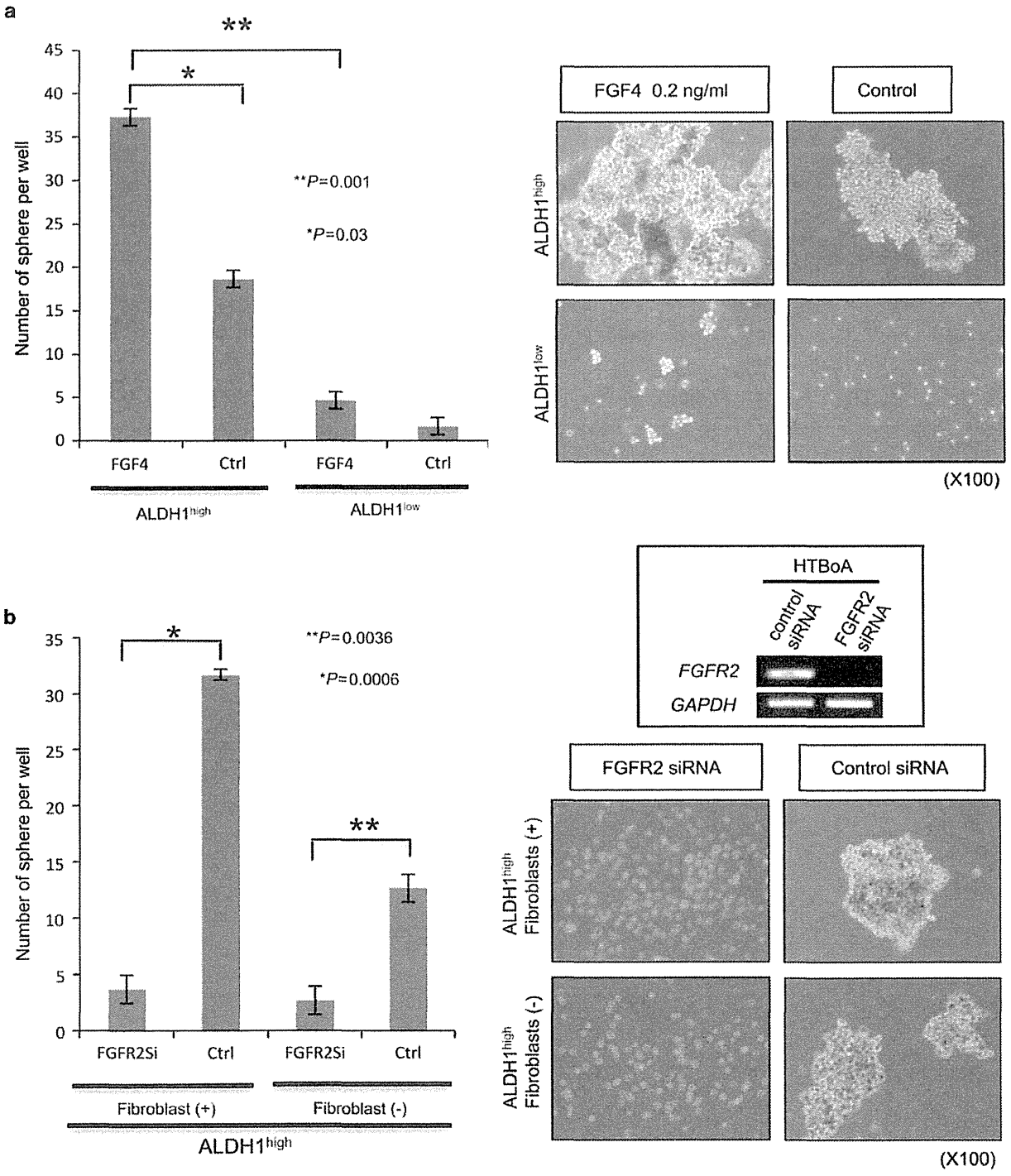

Figure 6 Sphere formation assay with recombinant FGF4 and FGFR2-siRNA. (**a**) Sphere formation assay with recombinant FGF4. Sphere-forming capacity of ALDH1^{high} cells and that of ALDH1^{low} cells were assessed. Recombinant human FGF4 was added to the sphere formation assay culture medium to a final concentration of 0.2 ng/ml. Data represent means ± s.d. The differences were examined for statistical significance using Student's *t*-test. **P*-values. Ctrl: PBS only. Representative sphere pictures are shown in the right panels (× 100). (**b**) Sphere formation assay with FGFR2 gene knockdown. Sphere-forming capacity was assessed after siRNA-mediated FGFR2 gene knockdown in ALDH1^{high} cells with or without a mixture of fibroblasts. Data represent means ± s.d. The differences were examined for statistical significance using Student's *t*-test. **P*-values. FGFR2Si: FGFR2-siRNA, Ctrl: control siRNA. FGFR2 gene knockdown was confirmed by RT-PCR (right upper panel). Representative sphere pictures are shown in the right lower panels (× 100).

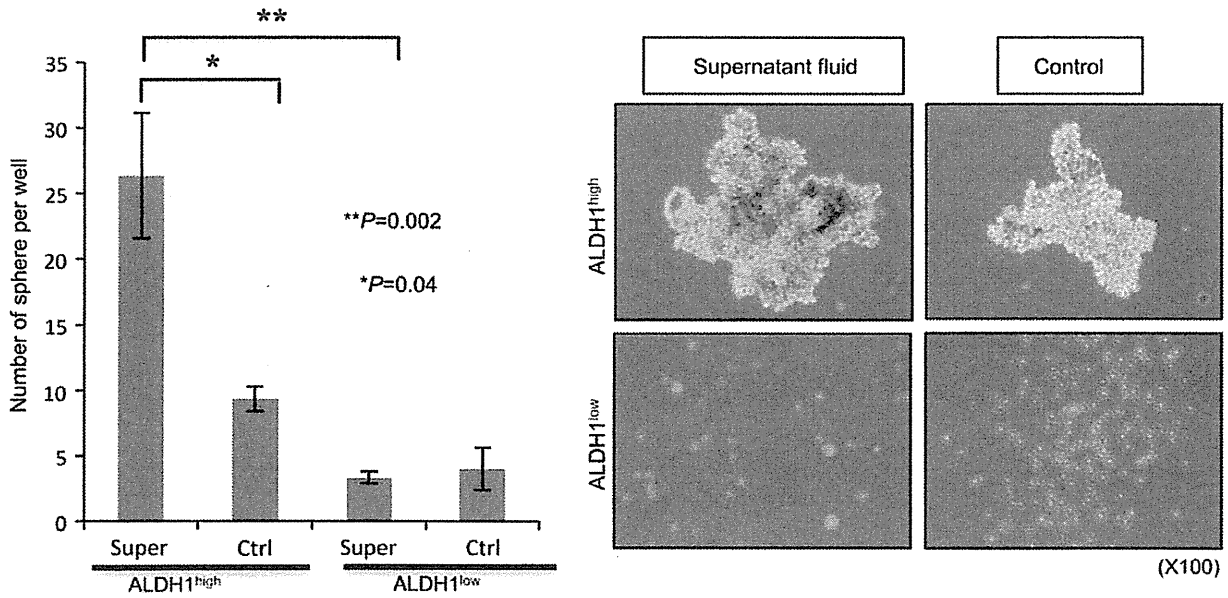

Figure 7 Sphere formation assay with fibroblast culture supernatant. Sphere-forming capacity of ALDH1^{high} cells and that of ALDH1^{low} cells were assessed. Fibroblast culture supernatant was added to the sphere formation assay culture medium to a final concentration of 50%. Data represent means ± s.d. The differences were examined for statistical significance using Student's *t*-test. **P*-values. Super: 50% fibroblast culture supernatant, Ctrl: medium only. Representative sphere pictures are shown in the right panels (× 100).

Table 3 Immunohistochemical analysis in 122 epithelial ovarian cancer tissues

All cases Characteristic	Score 0	Score 1	Score 2	Total	*P*-value
Patient No. (%)	44 (36.1)	53 (43.4)	25 (20.5)	122	
Mean age ± s.d. (years)	53.1 ± 10.11	56.4 ± 11.85	54.5 ± 9.73	54.8 ± 10.9	
Pathological subtype No. (%)					0.004
Serous	12 (19.4)	34 (54.8)	16 (25.8)	62	
Clear cell	24 (64.9)	7 (18.9)	6 (16.2)	37	
Endometrioid	7 (41.2)	9 (52.9)	1 (5.9)	17	
Mucinous	1 (16.7)	3 (50.0)	2 (33.3)	6	
FIGO stage No. (%)					<0.001
Stage I	27 (65.9)	10 (24.4)	4 (9.7)	41	
Stage II	4 (66.6)	1 (16.7)	1 (16.7)	6	
Stage III	13 (19.4)	40 (59.7)	14 (20.9)	67	
Stage IV	0 (0.0)	2 (25.0)	6 (75.0)	8	

(Table 3; Figure 8a): Score 0 (*FGF4* positivity; <5%), Score 1 (*FGF4* positivity; >5%, <10%) and Score 2 (*FGF4* positivity; >10%). The data were summarized in Table 3. FGF4 score 0 is significantly less in serous adenocarcinoma cases, and FGF4 score 1 is significantly higher in serous adenocarcinoma cases ($P = 0.004$). FGF4 score 0 is correlated with FIGO Stage I and score 2 is correlated with FIGO Stage IV ($P < 0.001$). The high expression of ALDH1 was correlated with poorer prognosis in previous study.[16] The correlation of FGF4 expression and ALDH1 expression was analyzed. There

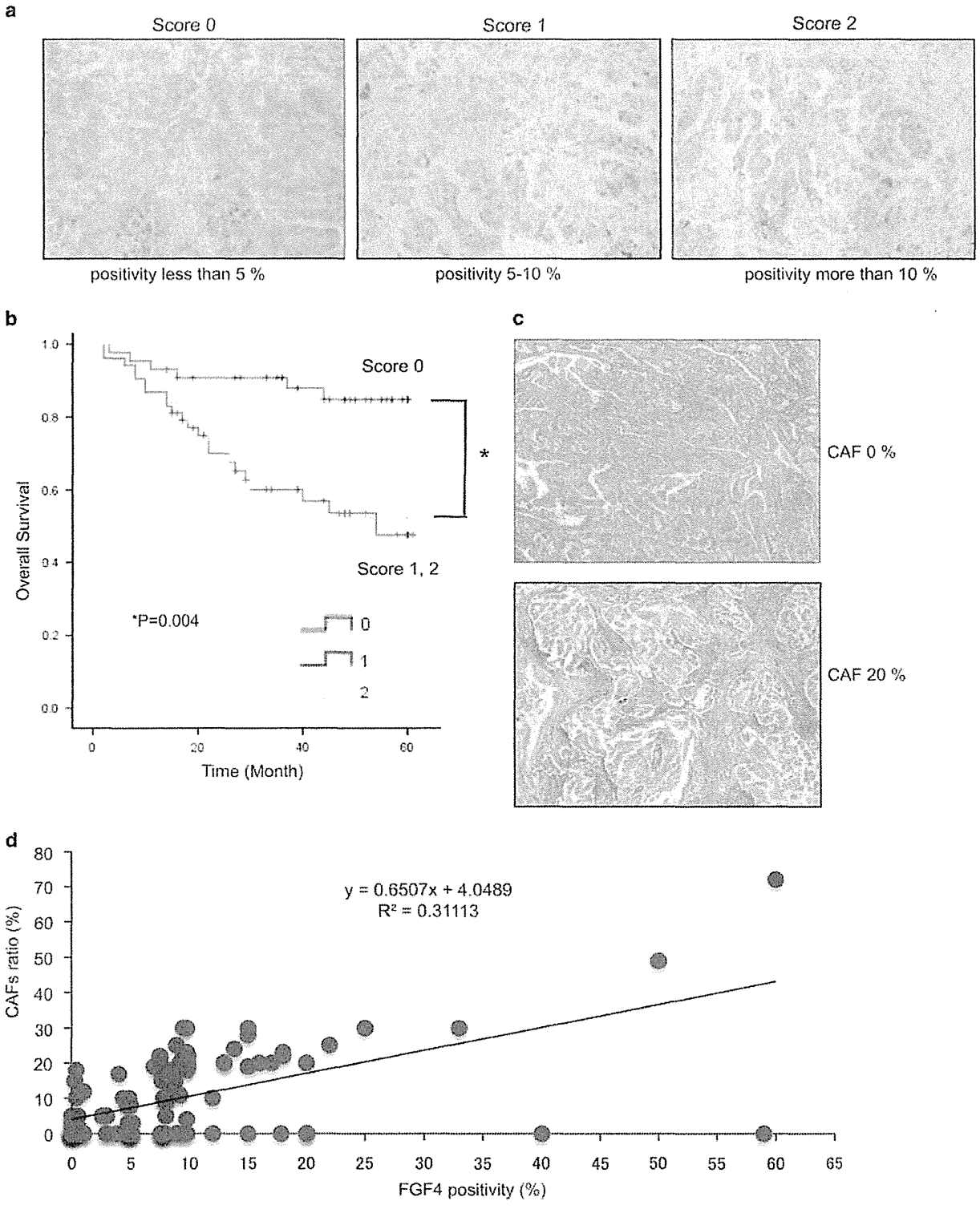

Figure 8 Correlation between FGF4 immunoreactivity and patients' clinical outcome or CAFs proportion. FGF4 immunoreactivity is associated with poor prognosis. (**a**) A total 122 of epithelial ovarian cancer tissues were immunohistochemically stained with anti-*FGF4* antibody and scored by three groups according to the positivity of staining. (**b**) The differences of overall survival were examined for statistical significance using Fischer's test. **P*-values. FGF4 immunoreactivity and CAFs ratio have certain correlation. (**c**) A total of 122 epithelial ovarian cancer tissues were stained with α-SMA antibody. (**d**) Each CAFs ratio and *FGF4* positivity rate were plotted and their correlation coefficient was analyzed by CORREL function.

were weak but significant correlation between FGF4-positive rates and ALDH1-positive rates ($r=0.234$, $P=0.009$) (Supplementary Figure 3). In Figure 8b, log-rank test revealed that higher expression of FGF4 (Score 1 and Score 2) is associated with poorer prognosis with a significant difference than those of lower expression levels of FGF4 ($P=0.004$). Higher expression levels of *FGF4* showed tendency with shorter PFS than those of lower expression levels of FGF4.

The Expression Level of *FGF4* and the Ratio of CAFs Have Certain Correlation

A total 122 of epithelial ovarian cancer tissues were also stained with α-SMA antibody and counted the positivity of staining as the ratio of CAFs (Figure 8c). The ratio of CAF and *FGF4* positivity rate were plotted and correlation coefficient was analyzed by CORREL function (Figure 8d). Correlation coefficient is 0.56. The expression level of *FGF4* and the ratio of CAFs are associated with significant correlation ($P<0.01$).

DISCUSSION

The cancer microenvironment has critical roles in cancer initiation, progression, invasion and metastasis, and CAF is a major component of the cancer microenvironment.[6] Actually, CAFs have roles in the adhesion and motility of tumor cells, and it is known that cancer cases with abundant CAFs have a poorer prognosis than that of cases with few CAFs.[9,11] Importantly, recent studies have indicated that stem-like phenotypes are more interactive with the cancer microenvironment. Therefore, we examined the interaction between fibroblasts and CSCs/CICs.

In the present study, we first demonstrated that highly tumorigenic CSCs/CICs could be isolated in an ALDH1^{high} population from HTBoA ovarian carcinoma cells. Previous studies showed successful isolation of ovarian CSCs/CICs by the ALDEFLUOR assay.[22] Therefore, the ALDEFLUOR assay is a promising approach to isolate ovarian CSCs/CICs. We next examined the action of fibroblasts on the tumor initiation capacity of CSCs/CICs and the histology of tumors. ALDH1^{high} tumors recruited prominent CAFs that were derived from recipient mice when inoculated with normal fibroblasts. Furthermore, a mixture with fibroblasts enhanced the expression of stem cell markers, *in vivo* tumor-initiating capacity and sphere-forming capacity of ALDH^{high} cells, indicating that cancer stem-like properties were upregulated by the action of fibroblasts.

RT-PCR analysis revealed that the *FGF4* gene was expressed in fibroblast-mixed ALDH1^{high} cells and tumor tissues. *FGF4* is known to have a key role in maintaining the self-renewal potential of normal stem cells such as trophoblastic stem cells.[23] Moreover, the role for *FGF4* of tumor invasion have also speculated.[23] We showed that *FGF4* could enhance the sphere-forming capacity of ALDH1^{high} cells, indicating that *FGF4* might be one of the growth factors mediating the stemness-promoting action of fibroblasts on CSCs/CICs. *FGF4* was initially isolated as an oncogene that could transform NIH3T3 cells.[20] *FGF4* gene amplification has been reported in various human cancers.[24–27] The *FGF4* gene is expressed from the early stage of embryonic development in fetal life and has essential roles in cell differentiation, morphogenesis and proliferation of a variety of organizations.[28] In human adult organs, *FGF4* is highly expressed in the testis. Thus, *FGF4* is one of key growth factors controlling proliferation and differentiation of normal stem cells or progenitor cells as well as cancer cells. In this study, we observed high FGF4 protein expression was correlated with poorer prognosis of ovarian cancer cases. Higher FGF4 expression rates were correlated with advanced stage and serous adenocarcinoma cases. Serous adenocarcinoma has high invasive feature than other histological subtypes, and invasion into stroma enables cancer cells to contact with CAFs physically.[29] Thus, invasion into stroma might be first step to induce FGF4-positive CSCs/CICs.

In our study, knockdown of *FGFR2*, a receptor for *FGF4* and other FGF family factors, almost completely inhibited sphere-forming capacity.[30] Therefore, it is thought that *FGFR2* signaling has a crucial role in the maintenance of cancer stemness properties such as sphere formation and *in vivo* tumor initiation in ovarian cancer HTBoA cells. *FGF4* production is induced in CSCs/CICs by stimulation of fibroblast-secreting factors and then *FGF4* promotes tumor initiation through autocrine and paracrine mechanisms (Figure 9). Interestingly, *FGF4* gene expression is controlled by transcription factors *POU5F1* (*Oct3/4*) and *Sox2*, which

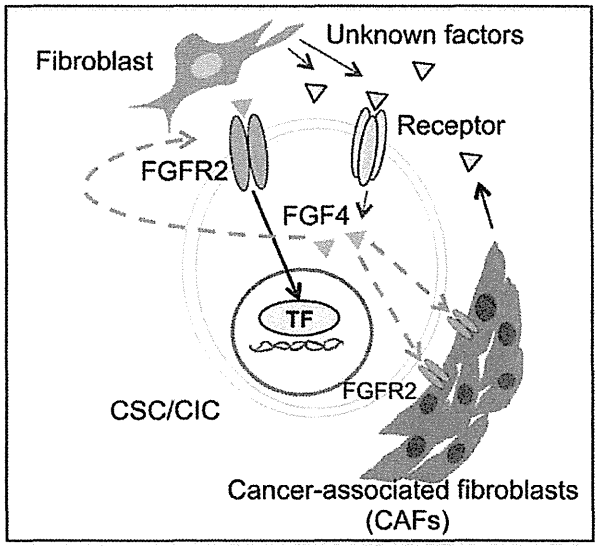

Figure 9 Working model of the role of FGF4-FGFR2 signaling in the interaction between CSCs/CICs and CAFs. Fibroblasts secrete unknown factors that stimulate FGF4 production in CSCs/CICs. FGF4 enhances the sphere-forming capacity and *in vivo* tumor initiation capacity by autocrine and paracrine mechanisms. FGF4 also recruits and activates CAFs.

are well-known cancer stem cell markers.[31] The results of the present study are consistent with these mechanisms, since both stem cell markers were upregulated in a fibroblast-mixed ALDH1^{high} tumor (Figure 4a). It should be noted, however, that other *FGFR2* ligands might also be produced in CSCs/CICs, since knockdown of *FGF4* could partially but not completely abrogate the stemness-promoting action of fibroblasts.

Various growth factors and cytokines produced from fibroblasts, including TGF-β,[8,32–34] have been reported to have important roles in the tumor microenvironment for promotion of the aggressiveness of cancer cells. Chao *et al*[13] reported that CD133$^+$ colon CSCs expressed high levels of *CXCR4* and were highly reactive to *SDF1*, which is secreted from CAFs. Tsuyada *et al*[35] reported that cancer cell-secreting cytokines stimulated production of *CCL2* in activated fibroblasts, which in turn activated Notch signaling and sphere-forming capacity in breast cancer stem cells. Thus, fibroblast-secreting factors have important roles in the maintenance of stem-like phenotypes and tumorigenicity of CSCs/CICs. It is important to identify the unknown fibroblast-secreting factors that induced *FGF4* expression in ovarian CSCs/CICs in our study. Such factors and *FGFR2* signaling might be potential targets for CSC/CIC-targeting therapy.

Supplementary Information accompanies the paper on the Laboratory Investigation website (http://www.laboratoryinvestigation.org)

ACKNOWLEDGMENTS

This study was supported by a Grant-in-Aid for Scientific Research from the Ministry of Education, Culture, Sports, Science and Technology of Japan (to NS, TT, JM and YH), program for developing the supporting system for upgrading education and research from the Ministry of Education, Culture, Sports, Science and Technology of Japan (to NS) and Takeda Science Foundation (to YH), Sagawa Foundation for Promotion of Cancer Research (to YH) and Suharakinennzaidann (to YH).

DISCLOSURE/CONFLICT OF INTEREST

The authors declare no conflict of interest.

1. Reya T, Morrison SJ, Clarke MF, *et al.* Stem cells, cancer, and cancer stem cells. Nature 2001;414:105–111.
2. Clarke MF, Dick JE, Dirks PB, *et al.* Cancer stem cells–perspectives on current status and future directions: AACR Workshop on cancer stem cells. Cancer Res 2006;66:9339–9344.
3. Clevers H. The cancer stem cell: premises, promises and challenges. Nat Med 2011;17:313–319.
4. Hirohashi Y, Torigoe T, Inoda S, *et al.* Immune response against tumor antigens expressed on human cancer stem-like cells/tumor-initiating cells. Immunotherapy 2010;2:201–211.
5. Park CY, Tseng D, Weissman IL. Cancer stem cell-directed therapies: recent data from the laboratory and clinic. Mol Ther 2009;17:219–230.
6. Allen M, Louise Jones J. Jekyll and Hyde: the role of the microenvironment on the progression of cancer. J Pathol 2011;223:162–176.
7. Pietras K, Ostman A. Hallmarks of cancer: interactions with the tumor stroma. Exp Cell Res 2010;316:1324–1331.
8. Orimo A, Gupta PB, Sgroi DC, *et al.* Stromal fibroblasts present in invasive human breast carcinomas promote tumor growth and angiogenesis through elevated SDF-1/CXCL12 secretion. Cell 2005;121:335–348.
9. Kalluri R, Zeisberg M. Fibroblasts in cancer. Nat Rev Cancer 2006;6:392–401.
10. Orimo A, Weinberg RA. Stromal fibroblasts in cancer: a novel tumor-promoting cell type. Cell Cycle 2006;5:1597–1601.
11. Kawase A, Ishii G, Nagai K, *et al.* Podoplanin expression by cancer associated fibroblasts predicts poor prognosis of lung adenocarcinoma. Int J Cancer 2008;123:1053–1059.
12. Aboussekhra A. Role of cancer-associated fibroblasts in breast cancer development and prognosis. Int J Dev Biol 2011;55:841–849.
13. Chao C, Carmical JR, Ives KL, *et al.* CD133+ colon cancer cells are more interactive with the tumor microenvironment than CD133- cells. Lab Invest 2012;92:420–436.
14. Ishiwata I, Ishiwata C, Soma M, *et al.* Establishment and characterization of a human ovarian anaplastic carcinoma cell line. Gynecol Oncol 1988;30:35–43.
15. Torigoe T, Asanuma H, Nakazawa E, *et al.* Establishment of a monoclonal anti-pan HLA class I antibody suitable for immunostaining of formalin-fixed tissue: unusually high frequency of down-regulation in breast cancer tissues. Pathol Int 2012;62:303–308.
16. Kuroda T, Hirohashi Y, Torigoe T, *et al.* ALDH1-high ovarian cancer stem-like cells can be isolated from serous and clear cell adenocarcinoma cells, and ALDH1 high expression is associated with poor prognosis. PLoS ONE 2013;8:e65158.
17. Yasuda K, Torigoe T, Morita R, *et al.* Ovarian cancer stem cells are enriched in side population and aldehyde dehydrogenase bright overlapping population. PLoS ONE 2013;8:e68187.
18. Giannoni E, Bianchini F, Masieri L, *et al.* Reciprocal activation of prostate cancer cells and cancer-associated fibroblasts stimulates epithelial-mesenchymal transition and cancer stemness. Cancer Res 2010;70:6945–6956.
19. Nishizawa S, Hirohashi Y, Torigoe T, *et al.* HSP DNAJB8 controls tumor-initiating ability in renal cancer stem-like cells. Cancer Res 2012;72:2844–2854.
20. Abate-Shen C, Shen MM. FGF signaling in prostate tumorigenesis–new insights into epithelial-stromal interactions. Cancer Cell 2007;12:495–497.
21. Sakamoto H, Mori M, Taira M, *et al.* Transforming gene from human stomach cancers and a noncancerous portion of stomach mucosa. Proc Natl Acad Sci USA 1986;83:3997–4001.
22. Wang YC, Yo YT, Lee HY, *et al.* ALDH1-bright epithelial ovarian cancer cells are associated with CD44 expression, drug resistance, and poor clinical outcome. Am J Pathol 2012;180:1159–1169.
23. Jordan NV, Johnson GL, Abell AN. Tracking the intermediate stages of epithelial-mesenchymal transition in epithelial stem cells and cancer. Cell Cycle 2011;10:2865–2873.
24. Szepetowski P, Courseaux A, Carle GF, *et al.* Amplification of 11q13 DNA sequences in human breast cancer: D11S97 identifies a region tightly linked to BCL1 which can be amplified separately. Oncogene 1992;7:751–755.
25. Jaakkola S, Salmikangas P, Nylund S, *et al.* Amplification of fgfr4 gene in human breast and gynecological cancers. Int J Cancer 1993;54:378–382.
26. Zaharieva BM, Simon R, Diener PA, *et al.* High-throughput tissue microarray analysis of 11q13 gene amplification (CCND1, FGF3, FGF4, EMS1) in urinary bladder cancer. J Pathol 2003;201:603–608.
27. Arao T, Ueshima K, Matsumoto K, *et al.* FGF3/FGF4 amplification and multiple lung metastases in responders to sorafenib in hepatocellular carcinoma. Hepatology 2012;57:1407–1415.
28. Yamamoto H, Ochiya T, Takahama Y, *et al.* Detection of spatial localization of Hst-1/Fgf-4 gene expression in brain and testis from adult mice. Oncogene 2000;19:3805–3810.
29. Behrens P, Rothe M, Florin A, *et al.* Invasive properties of serous human epithelial ovarian tumors are related to Ets-1, MMP-1 and MMP-9 expression. Int J Mol Med 2001;8:149–154.
30. Brooks AN, Kilgour E, Smith PD. Molecular pathways: fibroblast growth factor signaling: a new therapeutic opportunity in cancer. Clin Cancer Res 2012;18:1855–1862.

31. Katoh M, Katoh M. Comparative genomics on mammalian Fgf3-Fgf4 locus. Int J Oncol 2005;27:281–285.
32. Ikushima H, Miyazono K. TGFbeta signalling: a complex web in cancer progression. Nat Rev Cancer 2010;10:415–424.
33. Sigurdsson V, Hilmarsdottir B, Sigmundsdottir H, *et al.* Endothelial induced EMT in breast epithelial cells with stem cell properties. PLoS ONE 2011;6:e23833.
34. Scheel C, Eaton EN, Li SH, *et al.* Paracrine and autocrine signals induce and maintain mesenchymal and stem cell states in the breast. Cell 2011;145:926–940.
35. Tsuyada A, Chow A, Wu J, *et al.* CCL2 mediates cross-talk between cancer cells and stromal fibroblasts that regulates breast cancer stem cells. Cancer Res 2012;72:2768–2779.

Iwayama et al. World Journal of Surgical Oncology (2015) 13:36
DOI 10.1186/s12957-015-0456-2

WORLD JOURNAL OF SURGICAL ONCOLOGY

RESEARCH Open Access

Prognostic value of HLA class I expression in patients with colorectal cancer

Yuji Iwayama[1], Tetsuhiro Tsuruma[1*], Toru Mizuguchi[1], Tomohisa Furuhata[1], Nobuhiko Toyota[1], Masayuki Matsumura[1], Toshihiko Torigoe[2], Noriyuki Sato[2] and Koichi Hirata[1]

Abstract

Background: Prognostic factors are useful for determination of the therapeutic strategy and follow-up examination after curative operation in cancer treatment. The immunological state of the host can influence the prognosis for cancer patients as well as the features of the cancer. Human lymphocyte antigen (HLA) class I molecules have a central role in the anti-cancer immune system. Therefore, we focused on the HLA class I expression level in cancer cells to investigate its prognostic value in patients with colorectal cancer.

Methods: We reviewed the clinical pathology archives of 97 consecutive patients with stage II colorectal cancer who underwent curative operation at the Sapporo Medical University, Japan, from February 1994 to January 2005. Fifty-six high-risk patients had adjuvant chemotherapy. The cancer cell membrane immunoreactivity level for HLA class I expressed by EMR8-5 was classified into three categories (positive, dull, and negative). In this study, the cases were divided into two groups: "positive" and "dull/negative". HLA class I expression level and clinicopathological parameters were evaluated with the Pearson χ^2 test. Survival analysis was assessed by the Kaplan-Meier methods, and the differences between survival curves were analyzed using the log-rank test.

Results: Immunohistochemical study of HLA class I revealed the following. There were 51 cases that were positive, 40 were dull, and six negative. The HLA class I expression level had no significant correlation with other clinicopathological parameters, except for gender. Univariate and multivariate analyses related to disease-free survival (DFS) revealed that tumor location, HLA expression level, and venous invasion were significant independent prognostic factors ($P < 0.05$). The 5-year DFS rates in HLA class I positive group and in the dull/negative group were 89% and 70%, respectively. For high-risk patients with adjuvant chemotherapy, the 5-year DFS rates in the HLA class I positive group and in the dull/negative group were 84% and 68%, respectively. For low-risk patients without the chemotherapy, the
5-year DFS rates in the HLA class I positive group and in the dull/negative group were 100% and 71%, respectively.

Conclusions: Our study concluded that the HLA class I expression level might be a very sensitive prognostic factor in colorectal cancer patients with stage II disease.

Keywords: HLA class I, Colorectal cancer, Prognostic factor, Relapse, Disease-free survival

* Correspondence: tsuruma@sapmed.ac.jp
[1]Department of Surgery, School of Medicine, Sapporo Medical University, S1, W16, Chuo-ku, Sapporo, Hokkaido 060-0061, Japan
Full list of author information is available at the end of the article